

Analyst

Accepted Manuscript



This is an *Accepted Manuscript*, which has been through the Royal Society of Chemistry peer review process and has been accepted for publication.

Accepted Manuscripts are published online shortly after acceptance, before technical editing, formatting and proof reading. Using this free service, authors can make their results available to the community, in citable form, before we publish the edited article. We will replace this *Accepted Manuscript* with the edited and formatted *Advance Article* as soon as it is available.

You can find more information about *Accepted Manuscripts* in the [Information for Authors](#).

Please note that technical editing may introduce minor changes to the text and/or graphics, which may alter content. The journal's standard [Terms & Conditions](#) and the [Ethical guidelines](#) still apply. In no event shall the Royal Society of Chemistry be held responsible for any errors or omissions in this *Accepted Manuscript* or any consequences arising from the use of any information it contains.

ARTICLE

Single Gold Nanorod as Plasmon Resonance Energy Transfer Based Nanosensor for High Sensitive Cu(II) Detection

Cite this: DOI: 10.1039/x0xx00000x

C. Jing[‡], L. Shi[‡], X.-Y. Liu and Y.-T. Long*

Received 00th January 2012,
Accepted 00th January 2012

DOI: 10.1039/x0xx00000x

www.rsc.org/

Plasmon resonance energy transfer (PRET) has been widely applied in the detection of bio-recognition, heavy metal ions and cellular reactions with high sensitivity based on the overlap between plasmon resonance scattering band of nanoparticles and absorption band of surface modified chromophore molecules. Previous sensors based on PRET are all implemented on gold nanospheres with scattering light at the range of 530 to 600 nm. In this work, we developed a PRET based nanosensor on thiol-di(2-picolyl)amine modified single gold nanorod for the detection of Cu²⁺ ions in aqueous solution with high sensitivity and selectivity. Compared with nanospheres, gold nanorods with tunable and wide plasmon resonance bands from near-infrared to infrared region exhibit more promising potentials in acting as sensing probes.

Introduction

Plasmonic nanoparticles have been investigated and applied in many fields due to their surface plasmon resonance bands.¹ Particularly, gold nanoparticles (GNPs) with highly water-soluble and biocompatible properties are increasingly applied to construct sensors for biomolecules such as DNA, metal ions and cellular imaging.² Since the application of advanced optical instruments including dark-field microscopy (DFM), the scattering spectra of plasmonic nanoparticles were enabled to be monitored effectively at single nanoparticle level.³ Notably, in contrast to gold nanospheres, gold nanorod (GNR) sensors have shown larger spectral shifts and higher sensitivity on refractive index changes of the environment.⁴ Furthermore, while the resonance scattering bands of gold nanospheres are located in a narrow range from ca. 530 nm to ca. 600 nm, the plasmon resonance band of nanorods could be modulated in a wide range from near-infrared to infrared region by adjusting their aspect ratios.⁵ Therefore, GNRs with various size and optical resonance bands have been widely exploited in numerous fields including probing heavy metal ions, biological interaction, in vivo analysis, as well as photothermal therapy.⁶ In 2007, the phenomenon of plasmon resonance energy transfer (PRET) from gold nanospheres to surface modified Cytochrome c has been reported.⁷ PRET process occurs on the plasmonic nanoparticles with modified chromophore molecules. When the frequency of plasmon resonance band of metal nanoparticles is matched with the frequency of electronic absorption band of molecules, the resonance energy would

transfer from nanoparticles to the adsorbed molecules, resulting in the quenching of the plasmonic scattering spectra. The quantized quenching positions are exactly consistent with the absorption peaks of the chromophores. PRET provides an ultra-sensitive method for the detection of hundreds of molecules on the single nanoparticle surface. So far, it has been utilized to design high sensitive and selective probes due to that PRET only takes place when the frequency of the probe overlapped with the analytes.⁸ Copper is one of the essential elements for living organisms. However, long term exposure to a high level of copper can cause gastrointestinal disorders, liver or kidney diseases. In the past decades, considerable efforts have been made to detect Cu²⁺, such as optical and electrochemical methods.⁹ Particularly, most optical methods for the detection of copper ions are generally based on organic dyes. However, organic chromophores or fluorophores have limitations on sensitivity or low water solubility. To overcome these limitations, plasmonic nanoparticles have been used to construct optical sensors with high sensitivity in aqueous solutions. Previous works on PRET are mainly implemented on nanospheres with resonance bands at visible range less than 600 nm. It is worthy to note that nanorods with high scattering intensity and controllable peak wavelength could offer excellent nanoprobe for the PRET detection with high efficiency. It is readily to achieve the match of scattering band of plasmonics with the absorption band of surface modified chromophores. Herein, in this study, we observed PRET on the

Analyst Accepted Manuscript

gold nanorods for the first time and reported a PRET-based nanosensor for the determination of Cu^{2+} in aqueous solution. To construct the PRET sensor, we designed and synthesized a compound **TDPA** which has a thiol group (-SH) and a receptor di(2-picolyl)amine moiety (DPA) that has high affinity to Cu^{2+} with excellent selectivity. Furthermore, the sensor at single nanorod level provides high spatial resolution and sensitivity.

Experimental section

Reagents and materials

All reagents were of analytical grade. Gold chloride trihydrate ($\text{HAuCl}_4 \cdot 3\text{H}_2\text{O}$, >99.0%), sodium citrate, hydroxylamine hydrochloride, 2-Pyridinecarbaldehyde, pyridin-2-ylmethanamine, 1,2-dibromohexane, potassium thioacetate were purchased from sigma (USA). Absolute ethanol, acetone, $\text{CuSO}_4 \cdot 5\text{H}_2\text{O}$, $\text{Zn}(\text{NO}_3)_2$, $\text{Pb}(\text{NO}_3)_2$, $\text{Cd}(\text{NO}_3)_2$, CaSO_4 and other materials were purchased from Sinopharm Chemical Reagent Company (Shanghai, China). Gold nanorods (40 nm × 68 nm; 40 nm × 84 nm; 40 nm × 96 nm; 10 O.D.) were purchased from Nanoseedz (Hong Kong, China). Ultrapure water with a resistivity of 18.2 M Ω -cm was produced using a Milli-Q apparatus (Millipore, USA) and used in the preparation of all the solutions. The indium tin oxide (ITO) slides were purchased from Geao Co. Ltd. (Wuhan, China).

Preparation of the GNPs

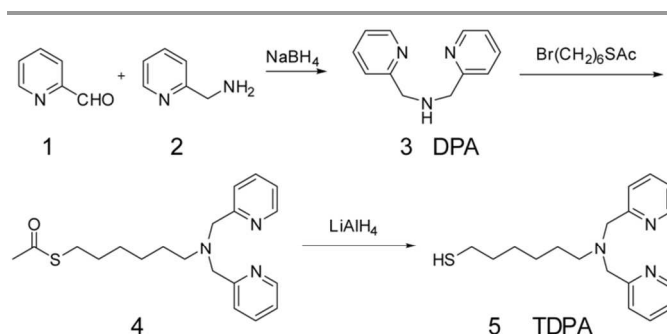
All glassware was immersed in an aqua regia solution (3:1 HNO_3/HCl) for 12 h (CAUTION: Aqua regia is strong acid and is highly corrosive; it should be handled with care) and then rinsed several times with ultrapure water before use. Seed GNPs with diameters of 13 nm were prepared according to a procedure that has been described previously.¹⁰ In brief, 50 mL of 0.01% wt% HAuCl_4 was added to a 100 mL round-bottom flask that was equipped with a condenser. The solution was brought to a rolling boil under vigorous stirring, and 5 mL of 38.8 mM sodium citrate was rapidly added to the vortex of the solution; the addition of sodium citrate caused the color to change from pale yellow to red. The solution was heated for 15 min and then stirred for an additional 15 min after the heating mantle had been removed.

The resulting solution of seed particles was used to prepare the larger gold particles using a procedure that has been described previously.¹¹ In brief, 25 mL of water, 1 mL of the solution of seed particles and 100 μL of 0.2 M $\text{NH}_2\text{OH} \cdot \text{HCl}$ were combined in a 50 mL beaker, and 3.0 mL of 0.1% wt% HAuCl_4 was added dropwise under vigorous stirring. As the HAuCl_4 solution was added, the color of the mixture gradually changed to dark red. The addition of the HAuCl_4 was completed within 5 min. The nanoparticle solutions were stored in dark bottles at 4 °C.

Preparation of TDPA

2-pyridinecarbaldehyde (2.51 g) was dissolved in 50 mL methanol, and pyridin-2-ylmethanamine (2.54 g) was added

dropwise under ice-bath condition. The mixture was stirred for 1 h at room temperature. After that, NaBH_4 (0.89 g) was added in portions at 0°C. The solution was stirred overnight, quenched with the addition of HCl, cooled with an ice-bath and then adjusted pH to 4. After remove the solvent, 25 mL H_2O was added to the residue. A solution of 1, 2-dibromohexane (6.00 g) and potassium thioacetate (1.40 g) in anhydrous THF (50 mL) was refluxed for 12 hours under argon. After cooling to room temperature, the KBr was removed by vacuum filtration. The solvent in the filtrate was removed under reduced pressure in a rotary evaporator. The residue was purified with column chromatography to give product **Br(CH₂)₆SAc**. To a solution containing **Br(CH₂)₆SAc** (0.24g), K_2CO_3 (0.276 g) and KI (0.033g) in 15 mL acetone was added dropwise a solution of **DPA 3** (0.298g) in 5 mL acetone. The mixture was stirred for 18h at 44 °C, then filtrated. The solvent was removed under vacuum, the residue was purified with column chromatography to give product **4**. To a solution of LiAlH_4 (0.17 g) in dry THF (5 mL) was added dropwise at 0°C a solution of **4** (0.357 g.) in dry THF (5 mL) over 15 min. The mixture was stirred for 4 h, and then poured into ice water (50 mL). The white precipitation was filtered. The water phase was extracted with CH_2Cl_2 (30 mL × 3). The organic phase was collected and dried with anhydrous Na_2SO_4 . The solvent was removed under vacuum. The crude product was purified with column chromatography to give product (**0.19 g**, 63%). The detailed synthetic routes are listed in Supporting Information.

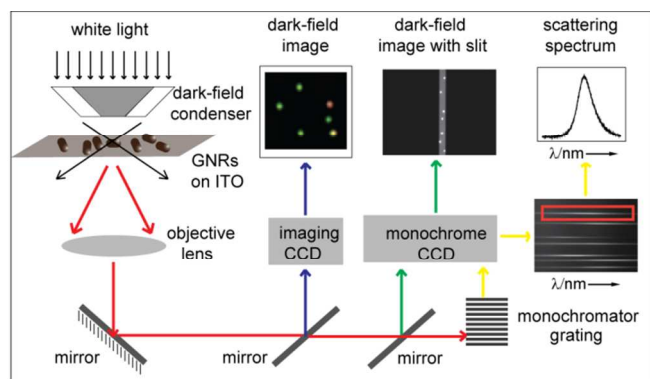


Scheme 1 Synthesis procedure of TDPA.

Preparation of the samples and setup

Gold nanoparticles used in the experiments were immobilized on the indium tin oxide (ITO) slides. The surfaces of ITO slides were cleaned in an ultrasonic bath in ethanol, acetone and water for more than 1 h in each solvent. The cleaned ITO slides were modified with GNPs via electrostatic adsorption by placing them in the diluted gold colloid solution (200 times) for 5 min. The GNP-functionalized ITO slides were then modified with the compound **TDPA** on the surface of GNPs via Au-S covalent bond after immersing ITO slide in 10 μM TDPA solution for 6 h. We have rinsed the sample with ethanol and water for several times to remove the TDPA with non-covalent bonding and dried under a stream of ultrapure nitrogen prior to the dark-field measurements. As shown in Scheme 2, the dark-

field measurements were carried out on an inverted microscope (eclipse Ti-U, Nikon, Japan) that was equipped with a dark-field condenser ($0.8 < \text{NA} < 0.95$) and a $40\times$ objective lens ($\text{NA} = 0.8$). A true-color digital camera (Nikon DS-fi, Japan) was used to capture the dark-field color images. The scattering light of gold nanoparticle was split by a monochromator (Acton SP2300i, Princeton Instruments, USA) and recorded by a spectrometer CCD (Pixis 400, Princeton Instruments, USA) to obtain the scattering spectra. The liquid exchange cell was made by PDMS. Additional details of the dark-field microscopy and spectroscopy setup have been reported in a previous work.³



Scheme 2 Setup of dark-field microscopy coupled with color CCD, spectrograph, spectro-CCD and slit which enables single nanoparticle detection.

Results and discussion

Effect of TDPA and copper ions on scattering spectra of GNRs

The DPA moiety has been widely applied in the construction of chemosensors for the determination of cations and anions.¹² After conjugation with Cu^{2+} , the TDPA- Cu^{2+} complex has a broad optical absorption band in the visible range (from 600 nm to 700 nm) and gives a blue solution (Fig. S1), this may be due to the 1:2 binding stoichiometry between Cu^{2+} and DPA ligand (Fig. 1A).^{9, 13} In order to enhance the PRET efficiency, single GNR with diameter 40 nm and length 68 nm with a scattering peak around 630 nm was used as nanoplasmonic probes due to the overlap between absorption of complex and scattering of nanoprobe (Fig. S1). The size of GNRs was characterized by SEM as shown in Fig. S2. The scattering images and spectra of individual TDPA-modified GNR were obtained by a dark-field microscopy coupled with spectrograph as shown in Fig. 1B-D. GNR exhibited a scattering peak around 630 nm with orange color, indicating that the modification of TDPA showed no obvious influence on scattering spectrum of GNR. However, upon the addition of Cu^{2+} , the selective energy transfer took place and the spectral resonant quenching on the Rayleigh scattering spectrum can be observed. The scattering spectra of GNR exhibit a substantial decrease in intensity without any noticeable spectral shift and the imaging brightness in dark-field also decreased. The scattering intensity decrease provided the basis for designing the nanosensor based on a single GNR.

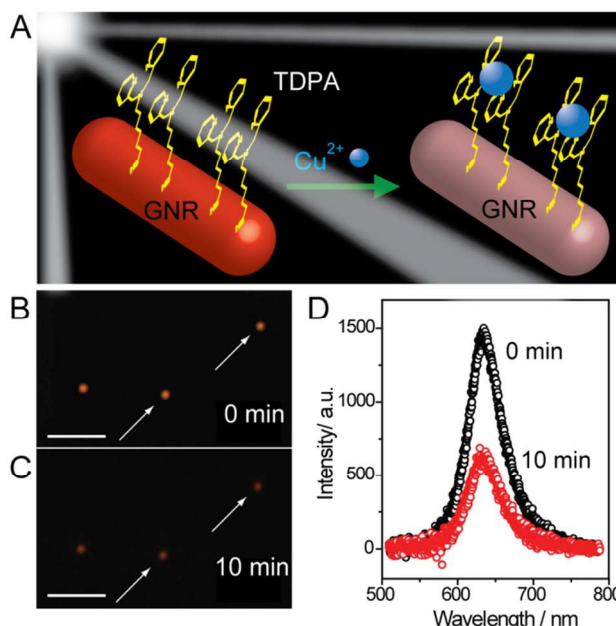


Fig. 1 (A) Schematic illustration of the nanosensor. The plasmonic signal intensity of gold nanorod is reduced by the formation of TDPA- Cu^{2+} ligand complex on the surface of single gold nanorod due to plasmon resonance energy transfer from nanorod to complex. (B-C) Dark-field images of gold nanorods before (B) and after (C) the treatment of 1 mM Cu^{2+} . (D) Corresponding scattering spectra changes of the plasmonic nanorod probe before (black) and after (red) exposure to 1 mM Cu^{2+} . The scale bar in B and C is 10 μm .

Time-dependent reaction and detection limit

Time-dependent scattering spectra intensity changes (ΔI) of the probe after exposure to 1 mM Cu^{2+} are shown in Fig. 2A. A single GNR probe exhibits up to 73.1% decrease in scattering intensity in 20 min. At the same time-interval, GNR did not show any scattering spectral intensity decrease in the absence of Cu^{2+} . Also, as expected, the addition of Cu^{2+} to bare GNR induced no noticeable change of the scattering spectra and dark-field images (Fig. S3). This means that the local refractive index change surrounding the GNRs has no obvious influence on the scattering intensity decrease. According to the mechanism of PRET, the main reason that leads to such spectral intensity decrease of the GNR should be attributed to the plasmon resonance energy transfer from GNR to the Cu^{2+} -ligand complex.

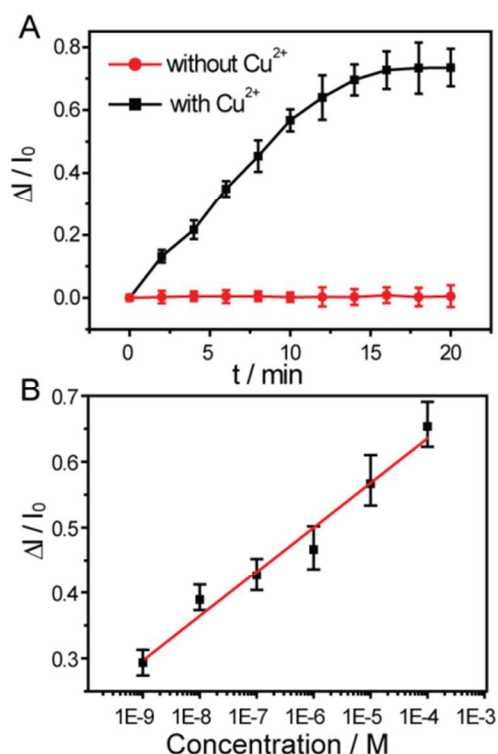


Fig. 2 (A) Representative time-dependent single TDPA-modified GNR scattering spectra intensity changes after treatment with Cu^{2+} (1 mM). (B) Equilibrium differential scattering intensity change of $\Delta I/I_0$ as a function of Cu^{2+} concentration. The red line is a logarithmic fitting of experimental data. The correlation coefficient is 0.99.

To investigate the sensitivity and applicability of this sensing system, changes in scattering intensity of GNR were determined after exposure to various concentrations of Cu^{2+} (10^{-9} – 10^{-4} M). As shown in Fig. 2B, the scattering intensity of the single TDPA-modified GNR decrease as the Cu^{2+} concentration increases. In addition, the changes of $\Delta I/I_0$ are found to be linear with the logarithm of Cu^{2+} concentration ranging from 10^{-9} to 10^{-4} M. It is remarkable that the scattering intensity of a single probe decreased about 30% after the exposure to 1 nM Cu^{2+} . The detection limit of 10^{-9} M confirms that the probe could be used to detect Cu^{2+} at ultratrace level showing high sensitivity.

Selectivity determination

As high selectivity is also crucial in real sample detection, the selectivity of this sensing system was evaluated by testing different biologically and environmentally relevant metal ions (K^+ , Na^+ , Pb^{2+} , Ni^{2+} , Zn^{2+} , Cd^{2+} , Ca^{2+} , Hg^{2+} , Mg^{2+}) at a concentration of 0.1 mM. As shown in Fig. 3, no obvious scattering quenching was observed after addition of these ions to our probe. However, the probe produces significant change in the scattering intensity upon exposure to 10 μM Cu^{2+} . These phenomena confirm the selectivity for Cu^{2+} over other ions even the transition metal ions despite that some ions could also complex with the DPA ligand. Only when the absorption profile of the metal-ligand complex matches the scattering spectrum of the probe, PRET process happens. This further

confirms that the sensing mechanism could indeed be a PRET process. In addition, the UV-Vis spectra of these ions with free TDPA in our previous work show that there are no changes around 600 nm to 700 nm in the presence of other ions as well as any blue color complex which confirmed the results.⁹

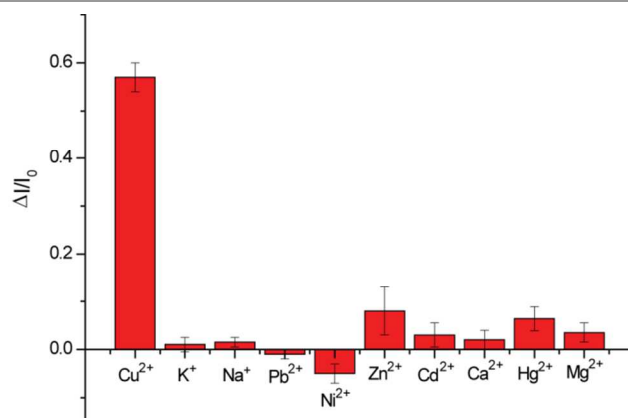


Fig. 3 Selectivity of the nanosensor for Cu^{2+} in the presence of K^+ , Na^+ , Pb^{2+} , Ni^{2+} , Zn^{2+} , Cd^{2+} , Ca^{2+} , Hg^{2+} , Mg^{2+} .

PRET efficiency of different GNPs

In addition, to confirm the PRET reliability and efficiency, different kinds of nanoparticles were exploited to observe the interaction between TDPA and copper ions. As shown in Fig. 4, 4 typical gold nanoparticles were modified with TDPA and treated with copper ions for 30 min. From the scattering spectra, it is clear that the nanosphere with peak wavelength of 592 nm exhibits only ca. 20% decrease in the scattering light intensity which is similar as the result of gold nanorod whose peak wavelength is at 730 nm, as shown in Fig. 4A and 4C. According to the UV-Vis spectrum of TDPA- Cu^{2+} complex in Fig. S2, the absorption intensity at these two positions are very low showing weak overlap with the scattering band of nanoparticles. In the contrast, the scattering spectra of gold nanorods with peak wavelength at 630 nm and 657 nm displayed obvious intensity decrease which is corresponding to the high absorption intensity. These results proved the process of PRET that more effective overlap between scattering band of plasmonic nanoparticles and absorption band of surface modified complex provides higher sensitivity of nanosensors. Furthermore, according to the mechanism of PRET, for the interference of complex with different absorption regions, the sensing selectivity could be enhanced by adjusting the scattering band of gold nanoparticles.

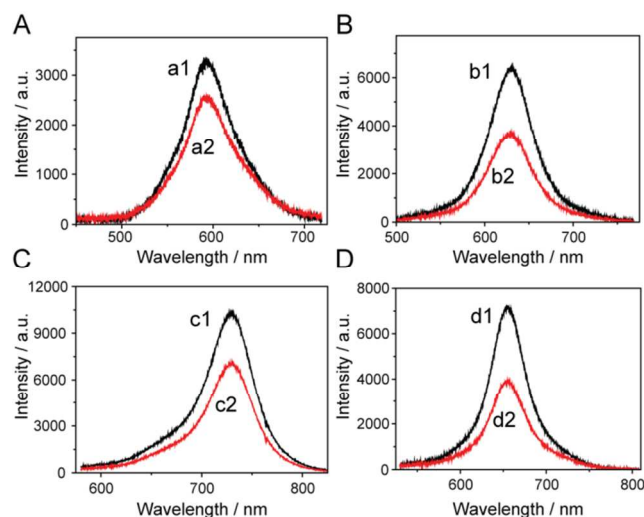


Fig. 4 Scattering spectra of TDPA modified gold nanospheres with peak wavelength of 592 nm (A) and gold nanorods with peak wavelength of 630 nm (B), 730 nm (C) and 657 nm (D) before (a1, b1, c1, d1) and after (a2, b2, c2, d2) the addition of 1 μM Cu^{2+} solution for 30 min. The nanorods with scattering bands at 657 nm and 730 nm are selected from nanoparticles of 40 nm \times 84 nm and 40 nm \times 96 nm, respectively.

Conclusions

In summary, we use scattering spectra of single GNR to develop a PRET-based sensing system for the first time for high sensitive and selective determination of Cu^{2+} in aqueous solution using a newly synthesized TDPA compound. Notably, GNRs with controllable aspect ratios showed wide range of plasmon resonance bands from near-infrared to infrared region which provide promising probes to match with different chromophores. Therefore, the PRET based method offered a novel way to detect heavy ions and other ligands through designing functional complex and adjusting the aspect ratios of nanorods.

Acknowledgements

This research was supported by 973 Program (2013CB733700), National Science Fund for Distinguished Young Scholars (21125522), Shanghai Pujiang Program (12JC1403500), Program for Professor of Special Appointment (Eastern Scholar) at Shanghai Institutions of Higher Learning (YJ0130504), and the National Natural Science Foundation of China (21327807).

Notes and references

Key Laboratory for Advanced Materials and Department of Chemistry, East China University of Science and Technology, Shanghai, 200237 P. R. China.

* To whom correspondence should be addressed:

Email: ytlong@ecust.edu.cn

† Electronic Supplementary Information (ESI) available: Experimental procedures and additional figures. See DOI: 10.1039/c000000x/

‡ These authors contributed equally to this work.

1 J. N. Anker, W. P. Hall, O. Lyandres, N. C. Shah, J. Zhao and R. P. Van Duyne, *Nat. Mater.*, 2008, **7**, 442-453; K. R. Catchpole and A.

- Polman, *Opt. Express*, 2008, **16**, 21793-21800; Y. Li, C. Jing, L. Zhang and Y.-T. Long, *Chem. Soc. Rev.*, 2012, **41**, 632-642; J. Ling and C. Z. Huang, *Anal. Methods*, 2010, **2**, 1439-1447; M. Segev-Bar, G. Shuster and H. Haick, *J. Phys. Chem. C*, 2012, **116**, 15361-15368.
- 2 S. Eustis and M. A. El-Sayed, *Chem. Soc. Rev.*, 2006, **35**, 209-217; D. A. Giljohann, D. S. Seferos, W. L. Daniel, M. D. Massich, P. C. Patel and C. A. Mirkin, *Angew. Chem. Int. Ed.*, 2010, **49**, 3280-3294; R. Elghanian, *Science*, 1997, **277**, 1078-1081; N. Gozlan, U. Tisch and H. Haick, *J. Phys. Chem. C*, 2008, **112**, 12988-12992; Z. Q. Yuan, J. Cheng, X. D. Cheng, Y. He and E. S. Yeung, *Analyst*, 2012, **137**, 2930-2932.
- 3 L. Zhang, Y. Li, D.-W. Li, C. Jing, X. Chen, M. Lv, Q. Huang, Y.-T. Long and I. Willner, *Angew. Chem. Int. Ed.*, 2011, **50**, 6789-6792; K. Li, W. Qin, F. Li, X. Zhao, B. Jiang, K. Wang, S. Deng, C. Fan and D. Li, *Angew. Chem. Int. Ed. Engl.*, 2013, **52**, 11542-11545; R. Vogelgesang and A. Dmitriev, *Analyst*, 2010, **135**, 1175-1181.
- 4 J. Becker, A. Trügler, A. Jakab, U. Hohenester and C. Sönnichsen, *Plasmonics*, 2010, **5**, 161-167; H. Chen, L. Shao, Q. Li and J. Wang, *Chem. Soc. Rev.*, 2013, **42**, 2679-2724.
- 5 Y. Huang and D.-H. Kim, *Nanoscale*, 2011, **3**, 3228-3232.
- 6 G. J. Nusz, S. M. Marinakos, A. C. Curry, A. Dahlin, F. Hook, A. Wax and A. Chilkoti, *Anal. Chem.*, 2008, **80**, 984-989; H. W. Huang, C. T. Qu, X. Y. Liu, S. W. Huang, Z. J. Xu, Y. J. Zhu, P. K. Chu, *Chem. Commun.*, 2011, **47**, 6897-6899; K. J. Lee, P. D. Nallathamby, L. M. Browning, T. Y. Desai, P. K. Cherukuri and X.-H. N. Xu, *Analyst*, 2012, **137**, 2973-2986.
- 7 G. L. Liu, Y.-T. Long, Y. Choi, T. Kang and L. P. Lee, *Nat. Methods*, 2007, **4**, 1015-1017.
- 8 Y. Choi, Y. Park, T. Kang and L. P. Lee, *Nat. Nanotechnol.*, 2009, **4**, 742-746; Y. Choi, T. Kang and L. P. Lee, *Nano Lett.*, 2008, **9**, 85-90; W.-G. Qu, B. Deng, S.-L. Zhong, H.-Y. Shi, S.-S. Wang, A.-W. Xu, *Chem. Commun.*, 2011, **47**, 1237-1239.
- 9 K. M. K. Swamy, S.-K. Ko, S. K. Kwon, H. N. Lee, C. Mao, J.-M. Kim, K.-H. Lee, J. H. Kim, I. Shin, J. Y. Yoon, *Chem. Commun.*, 2008, 5915-5917; Y.-Q. Weng, F. Yue, Y.-R. Zhong and B.-H. Ye, *Inorg. Chem.*, 2007, **46**, 7749-7755; H. Wang, L. Yang, W. Zhang, Y. Zhou, B. Zhao and X. Li, *Inorg. Chim. Acta*, 2012, **381**, 111-116; M. Li, H. Zhou, L. Shi, D. W. Li and Y. T. Long, *Analyst*, 2014, **139**, 643-648; A. Lee, J. W. Chin, O. K. Park, H. J. Chung, J. W. Kim, S.-Y. Yong, K. Park, *Chem. Commun.*, 2013, **49**, 5969-5971.
- 10 K. C. Grabar, R. G. Freeman, M. B. Hommer and M. J. Natan, *Anal. Chem.* 1995, **67**, 735-743.
- 11 S. Link, M. A. El-Sayed, *J. Phys. Chem. B* 1999, **103**, 4212-4217.
- 12 S. C. Burdette, C. J. Frederickson, W. Bu and S. J. Lippard, *J. Am. Chem. Soc.*, 2003, **125**, 1778-1787; A. Ojida, I. Takashima, T. Kohira, H. Nonaka and I. Hamachi, *J. Am. Chem. Soc.*, 2008, **130**, 12095-12101.
- 13 S. Youngme, K. Poopasit, K. Chinnakali, S. Chantrapromma and H.-K. Fun, *Inorg. Chim. Acta*, 1999, **292**, 57-63.